Proteomic Analysis of Lysosomal Acid Hydrolases Secreted by Osteoclasts

IMPLICATIONS FOR LYTIC ENZYME TRANSPORT AND BONE METABOLISM*

Cornelia Czupalla‡, Hannu Mansukoski‡, Thilo Riedl‡, Dorothee Thiel‡, Eberhard Krause§, and Bernard Hoflack‡¶

Osteoclasts, the bone-digesting cells, are polarized cells that secrete acid hydrolases into a resorption lacuna where bone degradation takes place. The molecular mechanisms underlying this process are poorly understood. To analyze the nature of acid hydrolases secreted by osteoclasts, we used the mouse myeloid Raw 264.7 cell line that differentiates *in vitro* into mature osteoclasts in the presence of the receptor activator of NF-κB ligand. Upon differentiation, we observed a strong increase in the secretion of mannose 6-phosphate-containing acid hydrolases. A proteomic analysis of the secreted proteins captured on a mannose 6-phosphate receptor affinity column revealed 58 different proteins belonging to several families of acid hydrolases of which 16 are clearly involved in bone homeostasis. Moreover these acid hydrolases were secreted as proproteins. The expression of most of the identified acid hydrolases is unchanged during osteoclastogenesis. Thus, our data strongly support the notion that the polarized secretion of acid hydrolases by osteoclasts results from a reorganization of key steps of membrane traffic along the lysosomal pathway rather than from a fusion of lysosomes with the membrane facing the resorption lacuna. *Molecular & Cellular Proteomics 5:134–143, 2006.*

Osteoclasts are the bone-resorbing cells involved in the tightly regulated process of bone remodeling. These multinucleated cells are formed by the fusion of mononuclear progenitors of monocyte/macrophage origin (1). Proliferation of the precursor cells and their differentiation into mature osteoclasts are essentially driven by two hematopoietic factors, macrophage colony-stimulating factor and receptor activator of NF-κB ligand (RANKL),[1] respectively (2). Activation of the corresponding receptors present at the cell surface of osteoclast precursors results in the regulated expression of a plethora of genes, including those encoding tartrate-resistant acid phosphatase (TRAcP), cathepsin K, and $\alpha_v\beta_3$ integrin that typify osteoclasts. Many of the corresponding gene products are required for reorganizing several key cellular functions such as cell adhesion, cytoskeleton dynamics, cell polarity, and membrane traffic along osteoclast differentiation. To digest bone, osteoclasts attach onto the bone surface, polarize, and create a specialized highly convoluted membrane domain, *i.e.* the ruffled border membrane that faces the bone surface thereby forming a sealed resorption lacuna (3). This resorption pit is acidified by vacuolar ATPases present on the ruffled border membrane leading to the breakdown of inorganic bone matrix mainly consisting of calcium hydroxyapatite (4, 5). In contrast, the digestion of the organic bone matrix, mostly made of collagens, proteoglycans, and other glycoproteins, requires the secretion of different acid hydrolases, in particular proteases, glycosidases, and sulfatases, most of them not identified yet.

Acid hydrolases are mainly soluble glycoproteins that, after synthesis as preproproteins in the endoplasmic reticulum, acquire a mannose 6-phosphate (Man-6-P) sorting marker on their *N*-linked oligosaccharides. This marker is recognized by two types of mannose 6-phosphate receptors (MPRs) that sort the acid hydrolases within the trans-Golgi network, the last sorting station of the secretory pathway (6). Resulting transport intermediates containing ligand-bound MPRs fuse with endosomes where the MPRs release their cargo. Acid hydrolases are then transported to and stored in lysosomes where they lose the Man-6-P marker and, in many cases, their prosequence to become mature, fully active enzymes. How acid hydrolases are secreted into the resorption lacuna of osteoclasts is not entirely clear yet. In early morphological studies a co-distribution of MPRs and some acid hydrolases along the secretory pathway from the site of biosynthesis to the ruffled border membrane has been shown, thus proposing a constitutive pathway for acid hydrolase secretion (7). Furthermore in more recent morphological studies lysosomal membrane glycoproteins, such as lgp110 and lamp2 as well as the vacuolar ATPase α3 subunit characteristic for late endosomes/lysosomes, were detected in the ruffled border membrane (8–10). This led to the proposal that late endocytic compartments, namely late endosomes and lysosomes, can

From the ‡Technical University of Dresden, 01307 Dresden, Germany and the §Institute of Molecular Pharmacology, 13125 Berlin, Germany

Received, September 8, 2005

Published, MCP Papers in Press, October 8, 2005, DOI 10.1074/mcp.M500291-MCP200

[1] The abbreviations used are: RANKL, receptor activator of NF-κB ligand; Cap, capillary; Man-6-P, mannose 6-phosphate; MPR, mannose 6-phosphate receptor; TRAcP, tartrate-resistant acid phosphatase; Z, benzyloxycarbonyl.

fuse with the membrane of the ruffled border thereby releasing their content of mature, fully active acid hydrolases into the resorption lacuna (11).

In the present study, we analyzed the secretion of acid hydrolases by osteoclasts in detail. We observed a strong increase in the secretion of different acid hydrolases, which still contained the Man-6-P targeting signal. Thus, we applied immobilized, cation-independent MPRs as highly specific affinity reagents for the purification of the complete set of Man-6-P-containing acid hydrolases and associated proteins secreted by osteoclasts. We present an exhaustive list of ≈60 proteins identified by MS, many of them being implicated in bone homeostasis. Our analysis further revealed that these Man-6-P-modified acid hydrolases are secreted as proforms thus suggesting a modification of MPR trafficking pathways during osteoclastogenesis.

EXPERIMENTAL PROCEDURES

Cell Culture and Metabolic Labeling—Soluble recombinant RANKL was produced in *Pichia* yeast as described previously (12). Raw 264.7 cells were obtained from American Type Culture Collection (Manassas, VA) and maintained in Dulbecco's modified Eagle's medium supplemented with 10% FCS (Hyclone Laboratories, Perbio Science, Erembodegem-Aalst, Belgium) and antibiotics. *In vitro* osteoclastogenesis was induced by addition of RANKL as described previously (12). Prior to collection of conditioned medium, cells were serum-starved for 6 h or overnight. For metabolic labeling, cells were incubated for 2 h with methionine-free Dulbecco's modified Eagle's medium containing 1 mCi/ml [^{35}S]methionine, 10 mM Hepes, pH 7.0, and 10% dialyzed FCS followed by a 3-h chase in the presence of 10 mM Man-6-P.

Immunoprecipitation of Cathepsin D—Conditioned medium from [^{35}S]methionine-labeled cells was diluted in lysis buffer (PBS supplemented with 0.5% Nonidet P-40, 0.5% sodium deoxycholate, and complete protease inhibitors (Roche Diagnostics)). Cells were washed twice with PBS, homogenized in lysis buffer, and centrifuged at 13,000 rpm for 15 min. Cell extracts and conditioned media were precleared with Protein A-Sepharose CL-4B (Amersham Biosciences), and cathepsin D was immunoprecipitated with a polyclonal antibody (13). Immunocomplexes were collected with Protein A-Sepharose and analyzed by SDS-PAGE followed by autoradiography.

Measurement of Enzyme Activities—For measurement of glycosidase activities, conditioned media were incubated for 3 h at 37 °C in assay buffer I (100 mM sodium citrate, pH 4.6, 0.2% Triton X-100) supplemented with a 1 mM concentration of the appropriate 4-methylumbelliferyl substrates. Reactions were stopped by addition of 0.5 M Na_2CO_3. Fluorescent reaction products were measured using a fluorescence multiwell plate reader (Tecan, Grödig, Austria) with excitation at 360 nm and emission at 440 nm. Cathepsin K activity was measured using (Z-Leu-Arg)$_2$-Rh110 bisamide (Calbiochem) in assay buffer II (100 mM sodium acetate, pH 5.5, 1 mM EDTA, 0.1 mM DTT). Reactions were terminated after 20 h at 37 °C by addition of 100 mM Tris, pH 8.0, 100 mM sodium iodoacetate, and fluorescence was measured at 485/530 nm. TRAcP activity was determined after dilution of conditioned media in HBSS buffer (118 mM NaCl, 4.6 mM KCl, 1 mM $CaCl_2$, 10 mM glucose, 20 mM Hepes, pH 7.2). Reactions were started by addition of assay buffer III (100 mM sodium acetate, pH 4.6, 40 mM sodium tartrate, 20 mM *p*-nitrophenyl phosphate) and stopped after 30 min at 37 °C by addition of 0.1 M NaOH. Colored reaction products were measured at 405 nm. Protein concentrations of corresponding cell extracts were determined using the DC protein assay (Bio-Rad), and enzymatic activities were normalized to the protein amount of the cells secreting these enzymes.

Purification of Man-6-P-containing Enzymes—Soluble bovine cation-independent MPR was purified from FCS by affinity chromatography on immobilized phosphomannan and coupled to Affi-Gel 15 (Bio-Rad) as described previously (14). Conditioned media were diluted in column buffer (50 mM imidazole, pH 6.5, 150 mM NaCl, 5 mM sodium β-glycerophosphate, 2 mM EDTA, 0.05% Triton X-100) and applied to an MPR Affi-Gel affinity column. The column was washed with 5 volumes of column buffer followed by 3 volumes of 5 mM glucose 6-phosphate in column buffer and 5 volumes of column buffer. Bound proteins were eluted with 5 volumes of 5 mM Man-6-P in column buffer and analyzed for their enzymatic activity or by SDS-PAGE.

Protein Identification by Mass Spectrometry—Proteins were separated by SDS-PAGE and visualized by staining with Coomassie Brilliant Blue. Protein bands were excised, washed, in-gel reduced, *S*-alkylated, and in-gel digested with trypsin (Promega, Madison, WI) as described previously (15). Peptides were extracted by addition of 0.3% trifluoroacetic acid in acetonitrile, the separated supernatant was dried under vacuum, and samples were redissolved in 0.1% (v/v) trifluoroacetic acid in water. MALDI-MS measurements were performed using an Ultraflex MALDI-TOF/TOF mass spectrometer (Bruker Daltonics, Bremen, Germany) in reflectron mode using α-cyano-4-hydroxycinnamic acid as matrix. All peptide mass fingerprint spectra were internally calibrated with trypsin autolysis peaks. MALDI-TOF/TOF fragment ion analysis was carried out in the LIFT mode of the instrument. Spectra were processed using FlexAnalysis software. Protein identification, both by peptide mass fingerprinting and fragment ion analysis, was performed using MASCOT (Matrix Science, London, UK). Search criteria were as follows: taxonomy, mouse; mass accuracy, 50 ppm for peptide mass fingerprinting and 0.5 Da for fragment analysis; modifications, carbamidomethylation and methionine oxidation; maximum one missed cleavage site. The National Center for Biotechnology Information (NCBI) non-redundant protein database (version 20041117; 2,171,938 sequences) and Swiss-Prot (version 45.5, 215,444 sequences) were searched. CapLC-MS/MS experiments were performed on the quadrupole orthogonal acceleration time-of-flight mass spectrometer Q-TOF Ultima (Micromass, Manchester, UK) equipped with a Z-spray nanoelectrospray source. A Micromass CapLC liquid chromatography system was used to deliver the peptide solution to the electrospray source. Peptides were separated using an analytical column (PepMap C_{18}, 3 μm, 100 Å, 150 mm × 75-μm inner diameter; LC Packings, Sunnyvale, CA) and an eluent flow rate of 200 nl/min. Mobile phase A was 0.1% formic acid (v/v) in acetonitrile-water (5:95, v/v), and B was 0.1% formic acid in acetonitrile-water (8:2, v/v). Runs were performed using a gradient of 3–64% B in 60 min. To perform MS/MS experiments automatic function switching (survey scanning) was used. The MS survey range was *m/z* 300–1990, and the scan duration was 1.0 s. The collision gas was argon at a pressure of 6.0×10^{-5} millibar. The MS/MS ion search option of the MASCOT program (www.matrixscience.com) was used to search against the NCBI non-redundant protein database and Swiss-Prot. The mass tolerance of precursor and sequence ions was set to 0.1 and 0.2 Da, respectively (other search criteria were as above).

Immunofluorescence and Confocal Laser Scanning Microscopy—Purified MPRs were fluorescently labeled with Alexa Fluor 488 (Molecular Probes, Eugene, OR). Raw 264.7 cells and osteoclasts grown on glass were fixed with 3% paraformaldehyde in PBS for 10 min and permeabilized in 0.05% saponin in PBS for 15 min. Samples were incubated with fluorescently labeled MPR fragments and primary anti-cathepsin D antibody in 1% bovine serum albumin in PBS for 1 h followed by incubation with Texas Red-conjugated goat anti-rabbit

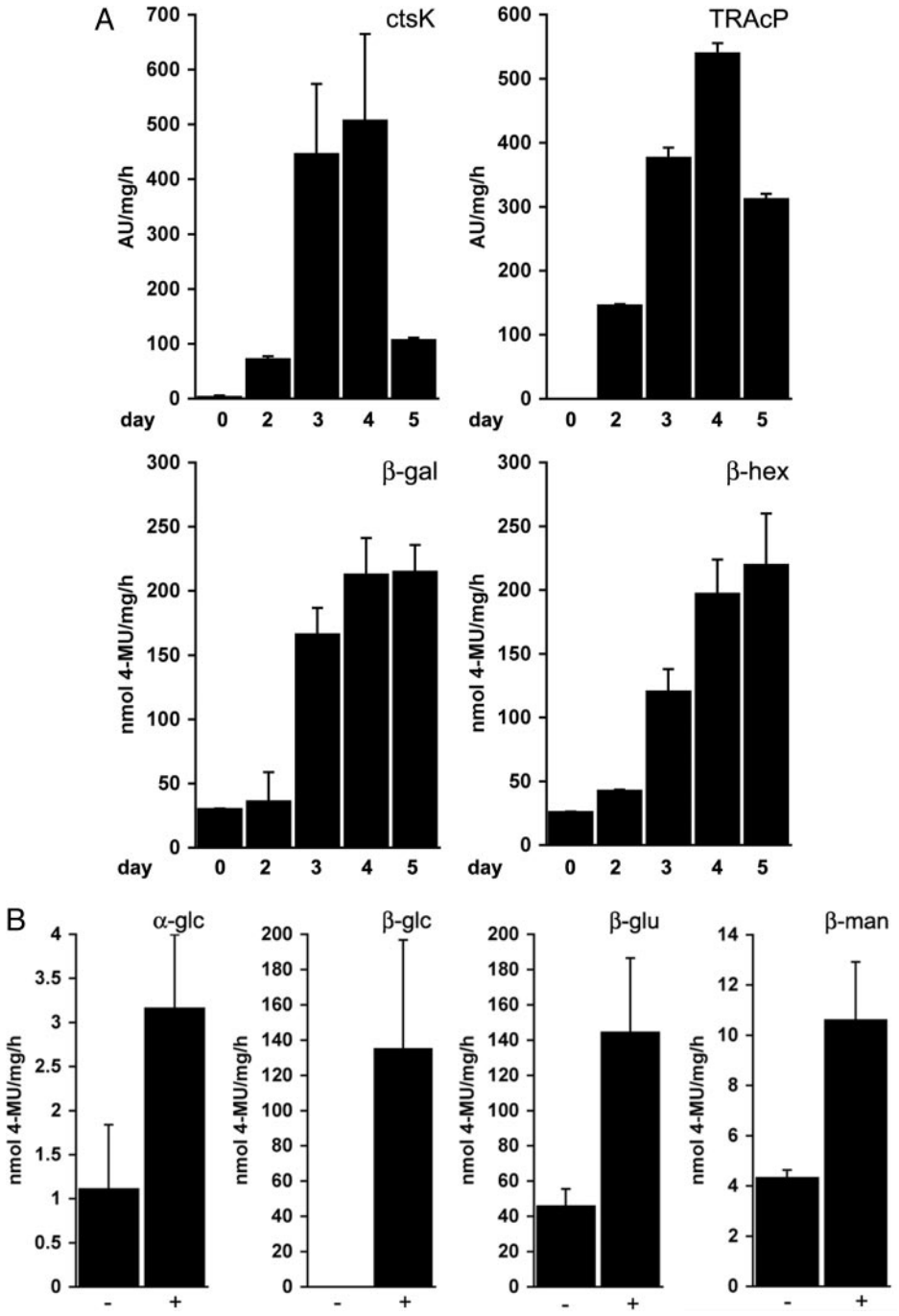

FIG. 1. **Secretion of acid hydrolases during osteoclastogenesis.** *A*, Raw 264.7 cells ($1.3 \times 10^4/cm^2$) were grown in the presence of RANKL for the times indicated. Conditioned media were collected from cells grown overnight in serum-free medium and assayed for TRAcP, cathepsin K (*ctsK*), β-galactosidase (*β-gal*), and β-hexosaminidase (*β-hex*). Enzymatic activities of conditioned media collected from non-treated Raw 264.7 cells did not change from day 0 to 5. *B*, Raw 264.7 cells were grown in the absence (−) or the presence (+) of RANKL for 5 days. Conditioned media were collected from cells grown in serum-deprived medium for 6 h and assayed for the indicated enzyme activities: α-glucosidase (*α-glc*), β-glucosidase (*β-glc*), β-glucuronidase (*β-glu*), and β-mannosidase (*β-man*). Enzyme activities were normalized to the total cellular protein (*A* and *B*). Shown are mean values ± S.D. of three independent experiments performed in duplicate. *4-MU*, 4-methylumbelliferone; *AU*, arbitrary units.

secondary antibody (Molecular Probes). Samples were viewed with a Zeiss LSM 510 Meta confocal laser scanning microscope (Zeiss, Jena, Germany).

DNA Microarray and Real Time PCR—mRNA isolation, cDNA synthesis, and Affymetrix expression analysis were done as described previously (12). Real time PCR was performed with a Stratagene Mx4000 QPCR system and Brilliant SYBR Green QPCR kit (Stratagene, La Jolla, CA) according to the manufacturer's instructions using the following primers: cation-dependent MPR, 5′-GGAATGGAGCAGTTTCCTCA-3′ and 5′-GGCAGGTTAGGGTCAAATCA-3′; cation-independent MPR, 5′-GCTGCTGCAGAAGAAGCTC-3′ and 5′-GTGATATGGCCATTTTCTTGC-3′; TRAcP, 5′-TTGTCAAGAACTTGCGACCA-3′ and 5′-TAGCGGACAAGCAGGACTCT-3′; cathepsin K, 5′-TGATGAAAATTGTGACCGTGA-3′ and 5′-CCTTCCAAAGCCACCAATATC-3′; cathepsin D, 5′-CCTGAAGCTAGGAGGCAAAA-3′ and 5′-AGGGTCCAGCAACACTAAGC-3′; legumain, 5′-TATGTGCTGGCCAATCTCTG-3′ and 5′-CCACCCAAACTGGCTTCTTA-3′; and β-glucuronidase, 5′-TGAATGGGATTCATGTGGTG-3′ and 5′-TGCTTGAAGCCTTTTTCTCC-3′.

RESULTS

Osteoclasts Secrete Acid Hydrolases Still Containing Mannose 6-Phosphate—As a model system of osteoclastogen-

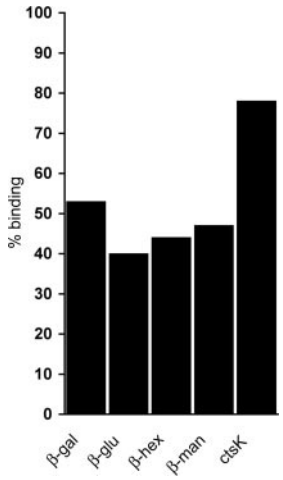

FIG. 2. **Osteoclasts secrete Man-6-P-modified acid hydrolases.** Raw 264.7 cells (1.3×10^4/cm^2) were treated with RANKL for 5 days to generate osteoclasts. Conditioned media collected from osteoclasts grown for 6 h in serum-free medium were passed over an MPR affinity column. The following enzymatic activities of the conditioned media as well as of the bound material eluted with 5 mM Man-6-P were determined: β-galactosidase (*β-gal*), β-glucuronidase (*β-gluc*), β-hexosaminidase (*β-hex*), β-mannosidase (*β-man*), and cathepsin K (*ctsK*). Shown are results from one representative experiment of three performed in duplicate.

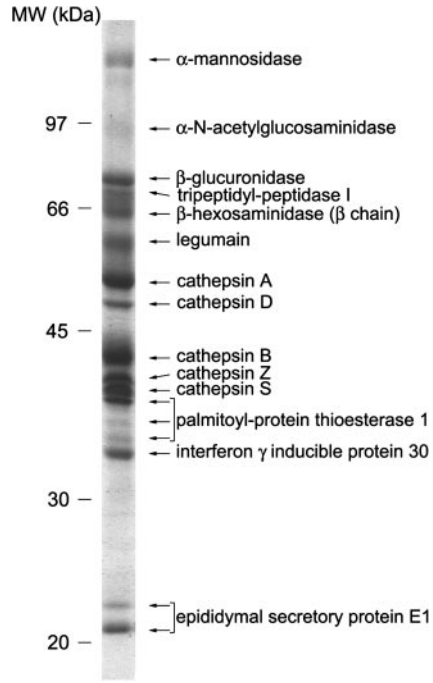

FIG. 3. **Protein profile of Man-6-P-containing proteins secreted by osteoclasts.** Raw 264.7 cells (1.0×10^7) were differentiated into osteoclasts in the presence of RANKL during 5 days and then grown overnight in serum-free medium. Conditioned medium was collected, and Man-6-P-containing proteins were purified on an MPR affinity column and separated by SDS-PAGE. Coomassie-stained bands were excised and analyzed by MALDI-TOF/TOF mass spectrometry. Molecular mass markers are indicated.

esis, we have used the mouse myeloid cell line Raw 264.7. Treatment of Raw 264.7 cells with RANKL for 4 days results in cultures mainly consisting of multinucleated osteoclasts (12, 16). We first followed the secretion of enzymatic activities of known acid hydrolases such as β-galactosidase and β-hexosaminidase as well as of the well characterized osteoclastogenesis markers cathepsin K and TRAcP (Fig. 1*A*). As expected, no secretion of cathepsin K and TRAcP was observed in precursor Raw 264.7 cells or during the early phase of differentiation. In contrast, secretion of both markers dramatically increased during later phases of differentiation when multinucleated osteoclasts were mostly present in the culture. Similarly we observed an increased secretion of β-galactosidase and β-hexosaminidase during osteoclastogenesis, reaching a maximum after 4 days of RANKL treatment. Osteoclasts secreted ≈10-fold more of both glycosidases than non-induced Raw 264.7 cells. Secretion of other acid hydrolases tested, such as α- and β-glucosidase, β-glucuronidase, and β-mannosidase, was also increased in osteoclasts (Fig. 1*B*).

Once in lysosomes, acid hydrolases lose the Man-6-P marker (17). Because efficient processing of acid hydrolases cannot be expected in the resorption lacunae of osteoclasts grown on plastic, retention of the Man-6-P targeting signal on acid hydrolases might indicate that these enzymes do not reach lysosomes before secretion. To investigate this, the acid hydrolases secreted into culture media of osteoclasts were tested for their capability to interact with purified MPRs immobilized on an affinity gel matrix. Fig. 2 shows that ≈80% of active cathepsin K interacted with immobilized MPRs, whereas ≈40–55% of the secreted β-galactosidase, β-glucuronidase, β-hexosaminidase, and β-mannosidase bound to the receptor. Thus, a significant fraction of these secreted enzymes still contains the Man-6-P marker as a typical hallmark of newly synthesized acid hydrolases.

Identification of Acid Hydrolases Secreted by Osteoclasts—Our results showing that several acid hydrolases are secreted as Man-6-P-containing proteins prompted us to identify the complete set of Man-6-P-modified proteins secreted by osteoclasts. Proteins were purified by their affinity to immobilized MPRs and further fractionated by SDS-PAGE as shown in Fig. 3. First the major Coomassie-stained bands were analyzed by peptide mass fingerprinting, and identified proteins were confirmed by MALDI-TOF/TOF peptide sequencing. This led to the identification of 14 proteins (see Fig. 3 and Table I). The major secreted Man-6-P-containing proteins are peptidases such as cathepsins A, B, D, S, and Z; legumain (asparaginyl endopeptidase); and tripeptidyl-peptidase I. Moreover glycosidases such as α-mannosidase, α-*N*-acetylglucosaminidase, β-hexosaminidase, and β-glucuronidase, enzymes involved in lipid metabolism, *i.e.* palmitoyl-protein thioesterase 1 and the epididymal secretory protein E1 (Niemann Pick C2 protein homolog), and another lysosomal protein, interferon γ-inducible protein 30 were found. To identify additional, less abundant Man-6-P-containing proteins, the gel

TABLE I
Proteins secreted by osteoclasts captured on an MPR affinity column

Protein	NCBI gene identifier	Predicted molecular mass	No. of sequenced peptides	Man-6-P	Propeptide sequence (position, MS/MS score)	Change in mRNA expression[a]	Bone phenotype (syndrome)
		Da					
Peptidases							
Dipeptidyl-peptidase I	3023454	52,343	10[b]	Yes	^{149}VNMNAAHLGGLQER^{162} (89), ^{167}LYTHNHNFVK^{176} (42), ^{184}SWTATAYK^{191} (35), ^{184}SWTATAYKEYEK^{195} (35)[b]	−2.7	Yes (Papillon-Lefevre, Haim-Munk)
Dipeptidyl-peptidase II	13626390	56,234	9[b]			1.3	
Tripeptidyl-peptidase I	12644085	61,304	12[b,c]	Yes	^{183}QRPEPQQVGTVSLHLGVT-PSVLR^{205} (44)[c]	1.3	
Retinoid-inducible serine carboxypeptidase	48474586	50,934	13[b]			−1.9	
Angiotensinase C-like	33469015	55,764	1[b,d]				
Cathepsin A	131082	53,809	13[b,c]	Yes			Yes (Goldberg)
γ-Glutamyl hydrolase	13124256	35,415	9[b]			−2.3	
Cathepsin Z	12585209	33,974	10[b,c]		^{31}SGQTCYHPIRGDQLALL-GR^{49} (45), ^{51}TYPRPHEYLSPADLP-K^{66} (45)[c]		
Cathepsin B	115712	37,256	11[b,c]	Yes	^{72}VAFGEDIDLPETFDAR^{87} (108)[c]	−1.8	
Cathepsin L	115742	37,523	12[b]	Yes	^{21}FDQTFSAEWHQWK^{33} (81), ^{38}RLYGTNEEEWR^{48} (32)[c]	−1.8	Yes
Cathepsin S	12643318	38,413	6[b,c]	Yes	^{29}DPTLDYHWDLWK^{40} (48), ^{29}DPTLDYHWDLWKK^{41} (54), ^{49}DKNEEEVR^{56} (49)[b]	−2.2	
Legumain	21617821	49,341	12[b,c]		^{324}TNDVKESQNLIGQIQQFLD-AR^{344} (80), ^{329}ESQNLIGQIQQFLDAR^{344} (51), ^{354}IVSLLAGFGETAER^{367} (59)[c]	−3.8	
Cathepsin K	12644320	36,865	8[b]	Yes	^{36}QYNSKVDEISR^{46} (30)[b]	8.4	Yes
Cathepsin F	12643321	51,628	6[b]		^{47}FALDMYNYGR^{56} (64), ^{244}SINDLAPPEWDWR^{256} (72)[b]	1.6	
Cathepsin D	115718	44,925	12[b,c]	Yes	^{35}TMTEVGGSVEDLILKGPITK^{54} (52)[c]	−1.4	
Glycosidases							
Di-*N*-acetylchitobiase	27229204	41,504	2[b]			−1.6	
Sialidase 1	17367967	44,563	5[b]	Yes			Yes
Lysosomal α-glucosidase	51338793	106,180	10[b]	Yes			
α-Galactosidase A	1703210	47,611	1[b,e]	Yes			
β-Galactosidase	114944	73,074	14[b]	Yes		3.2	Yes (Morquio)
Lysosomal α-mannosidase	17380364	114,532	34[b,c]	Yes		−1.6	Yes
Epididymis-specific α-mannosidase	17367999	115,551	31[b,c]			−1.8	Yes
β-Mannosidase	13310141	101,320	2[b]	Yes		1.6	Yes
β-Glucuronidase	114964	74,192	23[b,c]	Yes			Yes
β-Glucosidase	121284	57,585	2[b]	No			Yes (Gaucher)
α-*N*-*Acetylglucosaminidase*	7305299	82,115	4[b]	Yes		−1.3	Yes (Sanfilippo)
Tissue α-L-fucosidase	31541781	53,452	2[b]	Yes		−1.5	
β-Hexosaminidase α chain	232255	60,560	16[b]	Yes	^{37}YTLYPNNFQFR^{47} (47)[c]		
β-Hexosaminidase β chain	1346280	61,077	20[b,c]	Yes	^{31}LQPALWPFPR^{40} (47)[c]	1.8	
α-L-Iduronidase	1352424	71,135	11[b]	Yes			Yes (Hurler)
N^4-(β-*N*-Acetylglucosaminyl)-L-asparaginase	2498163	36,998	5[b]	Yes			
Sulfatases							
Galactosamine (*N*-acetyl)-6-sulfatase	31980654	57,989	4[b]	Yes			Yes (Morquio)
Arylsulfatase A	1703420	53,742	4[b]	Yes			
Arylsulfatase B	33302601	42,868	5[b]	Yes			Yes (Maroteaux-Lamy)
Glucosamine (*N*-acetyl)-6-sulfatase	29789239	62,042	5[b]	Yes		1.5	Yes (Sanfilippo)

TABLE I—*continued*

Protein	NCBI gene identifier	Predicted molecular mass	No. of sequenced peptides	Man-6-P	Propeptide sequence (position, MS/MS score)	Change in mRNA expression[a]	Bone phenotype (syndrome)
		Da					
N-Sulfoglucosamine sulfohydrolase	31543697	56,659	2[b]	Yes			Yes (Sanfilippo)
Lipid Metabolism							
Lysosomal phospholipase A_2	44888107	47,277	5[b]			−1.5	
Lysosomal acid lipase/cholesteryl ester hydrolase	20138798	45,521	8[b]	Yes		−3.5	
Lipoprotein lipase	417255	53,093	2[b]	No			
Sialate *O*-acetylesterase	25091741	60,724	3[b]				
Palmitoyl-protein thioesterase 1	20141662	34,467	10[b,c]	Yes		−1.4	
Palmitoyl-protein thioesterase 2	20138875	34,344	3[b]				
Acid sphingomyelinase-like phosphodiesterase 3a	18202337	49,807	3[b]			−3.1	
Sphingomyelin phosphodiesterase	1351982	69,882	3[b]	Yes		2.4	
Acid ceramidase	8134329	44,641	4[b]	Yes			
Epididymal secretory protein E1	14423831	16,432	5[b,c]	Yes		2.4	
Others							
Procollagen-lysine,2-oxoglutarate 5-dioxygenase 1	25008938	83,542	13[b]				Yes (Ehlers-Danlos)
Tartrate-resistant acid phosphatase type 5	730357	36,784	6[b]	Yes		530	
Deoxyribonuclease IIα	3182989	38,786	8[b]				
Ribonuclease T2	20139718	29,590	5[b]			3.5	
Interleukin-4-induced protein 1	3913652	70,147	4[b]				
Dentin matrix protein 4	56435263	64,405	2[b]			−2.4	
Prosaposin	3914939	61,381	10[b]	Yes		−1.3	
Interferon γ-inducible protein 30	15212492	27,794	2[c]	Yes			
Possible contaminants							
Lysozyme C, type P	126599	16,783	2[b]			−1.7	
β-1,4-Galactosyltransferase 5	13123982	44,701	3[b]			−1.8	
Polypeptide *N-acetyl-galactosaminyltransferase 6*	51315988	71,491	8[b]			1.4	
CMP-N-acetyl-neuraminate-poly-α-2,8-sialyltransferase	2494835	41,230	2[b]			1.4	

[a] Average -fold change ratio in Raw 264.7 cells *vs.* osteoclasts ($p < 0.05$).
[b] Peptide sequencing by LC-ESI-Q-TOF.
[c] Peptide sequencing by MALDI-TOF/TOF.
[d] Precursor ion, 537.27$[M + 2H]^{2+}$; sequence, K^{113}AMLVFAEHR^{121}Y; score, 72.
[e] Precursor ion, 545.30$[M + 2H]^{2+}$; sequence, R^{407}VNPSGTVLFR^{416}L; score, 51.

was cut into 50 slices of equal size, and each of them was subjected to protein identification by tryptic in-gel digestion followed by CapLC-ESI tandem mass spectrometry. Analysis of 11,191 MS/MS spectra revealed a total number of 58 different proteins belonging to several families of acid hydrolases including the known osteoclast markers cathepsin K and TRAcP (see Table I). This includes 15 peptidases, 16 glycosidases, five sulfatases, 10 enzymes involved in lipid metabolism, and 12 others. Among those, 33 proteins have been described previously as lysosomal acid hydrolases carrying the typical Man-6-P recognition marker such as cathepsins A, B, and D or α- and β-mannosidase (18). Our analysis also revealed lysosomal enzymes such as dipeptidyl-peptidase II, angiotensinase C-like protein, γ-glutamyl hydrolase, cathepsins F and Z, legumain, di-*N*-acetylchitobiase, and lysosomal phospholipase 2A for which a Man-6-P modification has not been described yet, indicating that they might be transported to lysosomes by a Man-6-P-dependent pathway in normal cells. Moreover we identified a third group of proteins that have not been classified as lysosomal acid hydrolases so far, namely sphingomyelinase-like phosphodiesterase 3a, interleukin-4-induced protein 1, and dentin matrix protein 4. It is interesting to note that β-glucosidase (β-glucocerebrosidase) and lipoprotein lipase, which do not contain Man-6-P residues, were also detected, probably reflecting their interaction with other Man-6-P-containing ligands. This probably holds true for four other proteins that are clearly not lysosomal enzymes, *i.e.* lysozyme C and three glycosyltransferases (*N*-acetylgalactosaminyltransferase 6, β-1,4-galactosyltransferase 5, and CMP-*N*-acetyl-poly-α-2,8-sialyltransferase), which were counted as possible contaminants. These glycosyltransferases are type II transmembrane proteins, which could

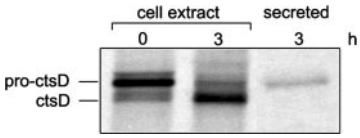

FIG. 4. **Cathepsin D is secreted as proenzyme.** Osteoclasts were metabolically labeled with [^{35}S]methionine for 30 min and then chased for 0 and 3 h. Cathepsin D (*ctsD*) was immunoprecipitated from cell extracts, and conditioned media and immunocomplexes were resolved by SDS-PAGE. Shown is one representative autoradiography of three. Molecular masses of cathepsin D precursor (55 kDa) and mature cathepsin D (45 kDa) are indicated.

be released as a soluble form after proteolytic cleavage.

To determine whether the Man-6-P-containing acid hydrolases were also secreted as proproteins, the MS/MS data were evaluated with respect to the presence of tryptic peptides overlapping with propeptide sequences. Although not all acid hydrolases contain a propeptide, such prosequences were found for 12 acid hydrolases, in particular for peptidases such as cathepsins B, D, F, K, L, S, and Z; dipeptidyl-peptidase I; tripeptidyl-peptidase I; and legumain as well as for β-hexosaminidase α and β chains (see Table I). For some other prosequence-containing acid hydrolases such as dipeptidyl-peptidase II, β-galactosidase, and lysosomal α-glucosidase we were not able to identify tryptic peptides spanning the propeptide sequence because they were either too short or too long to be detected by MS. Angiotensinase C was identified with only one peptide, which did not overlap with the prosequence. The other identified acid hydrolases are known not to contain a propeptide.

To confirm the finding that osteoclasts secrete proforms of acid hydrolases, we metabolically labeled osteoclasts and immunoprecipitated cathepsin D, one of the major secreted Man-6-P-containing proteins from cell extracts and conditioned media. Fig. 4 shows that cathepsin D is synthesized as a ≈55-kDa proform that is maturated into a 45-kDa form in murine osteoclasts. In contrast, secreted cathepsin D was exclusively detected as 55-kDa proform. This is in accordance with our MS/MS analysis of the propeptide sequence of cathepsin D and further underlines that acid hydrolases are secreted as proforms by osteoclasts. The presence of mature 45-kDa cathepsin D in intracellular compartments implicates that the enzyme reaches acidic compartments, *i.e.* late endosomes/lysosomes in osteoclasts. Indeed we also analyzed the intracellular distribution of cathepsin D in precursor Raw 264.7 cells and osteoclasts and compared it with the pattern of Man-6-P-modified proteins. For that purpose we fluorescently labeled a soluble form of MPRs. With this probe we detected Man-6-P-containing proteins mostly in perinuclear compartments, presumably Golgi structures, both in Raw 264.7 cells and osteoclasts (Fig. 5). Moreover more peripheral structures reminiscent of endosomes were labeled with the fluorescent MPR probe in osteoclasts. Binding of the MPR probe was quenched by the addition of 10 mM Man-6-P, thus proving the specificity of the detection of Man-6-P-containing proteins (data not shown). Cathepsin D was detected in scattered intracellular compartments both in precursor cells and osteoclasts. Only part of the cathepsin D-positive structures also contained Man-6-P-modified proteins, but a significant cathepsin D staining was also seen in structures that are clearly not labeled with the fluorescent MPR probe. This indicates that cathepsin D reaches acidic compartments where it loses the Man-6-P modification both in Raw 264.7 cells and osteoclasts. Taken together, our data suggest that two pools of cathepsin D and probably other acid hydrolases exist in osteoclasts, one of which is delivered to lysosomes and matures in this compartment, whereas the other is directly transported to the ruffled border and secreted as Man-6-P-modified proproteins.

Expression Levels of Acid Hydrolases and MPRs during Osteoclastogenesis—Our finding of a drastic increase in secretion of Man-6-P-containing proteins during osteoclastogenesis could be explained by an increase in the expression levels of at least some of these proteins, which could result in an overload of the receptors in the trans-Golgi network. On the other hand, down-regulation of MPRs could explain the increased secretion of acid hydrolases. Therefore, expression of both MPRs, *i.e.* cation-dependent and cation-independent Man-6-P receptors, was analyzed in Raw 264.7 cells and osteoclasts by quantitative real time PCR. Table II shows that the expression of neither of the receptors was significantly changed during osteoclastogenesis. This is in accordance with our DNA microarray analysis of mRNA expression in osteoclasts (12). Similarly the mRNA expression levels of most of the secreted acid hydrolases were not dramatically increased. Some Man-6-P-modified proteins such as dipeptidyl-peptidase I, legumain, and lysosomal acid lipase were even expressed at lower levels in osteoclasts (see Table I). These findings were confirmed by quantitative real time PCR analysis of selected gene products (see Table II). The only exceptions are the two known osteoclast markers cathepsin K and TRAcP, which are expressed at much higher levels in osteoclasts but are not major secreted proteins (see Fig. 3). Therefore, it is not likely that increased secretion of acid hydrolases is caused by their increased expression or by changes in the expression of the MPRs.

DISCUSSION

The results of our present study show that osteoclasts acquire the property of secreting large amounts of Man-6-P-containing precursor forms of acid hydrolases during their differentiation process. In our proteomic analysis, we captured Man-6-P-modified proteins secreted by osteoclasts on immobilized MPR affinity columns and thus could analyze the complete set of Man-6-P-containing acid hydrolases and associated proteins involved in bone degradation. We identified ≈60 proteins that mostly belong to the subfamilies of peptidases, glycosidases, sulfatases, and enzymes involved in lipid

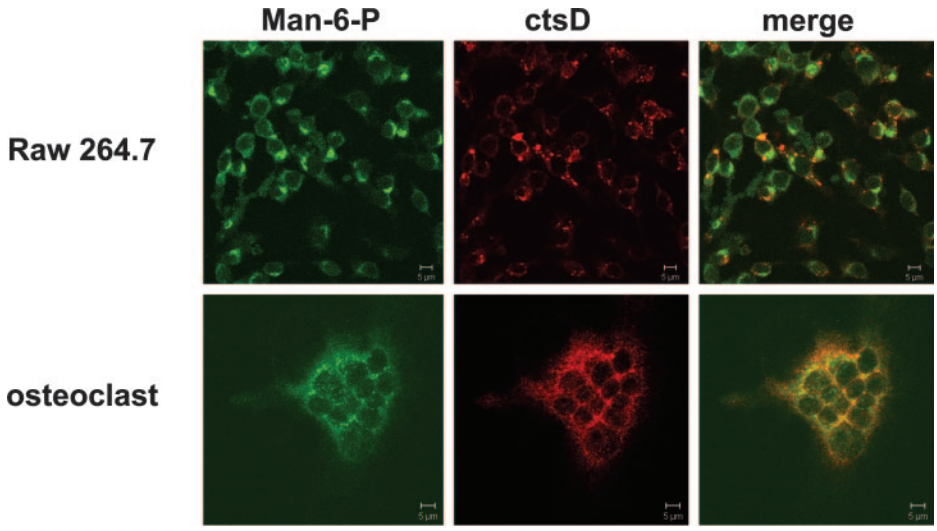

FIG. 5. **Distribution of Man-6-P-containing proteins and cathepsin D in precursor cells and osteoclasts.** Raw 264.7 cells and osteoclasts grown on glass were fixed, permeabilized, and stained with fluorescently labeled MPR fragments (*Man-6-P*, *green*) and anti-cathepsin D antibody (*ctsD*, *red*). Specimens were analyzed by confocal microscopy.

TABLE II
Changes in gene expression during osteoclastogenesis detected by real time PCR

Gene	-Fold change[a]
Cation-dependent MPR	1.59 ± 0.32
Cation-independent MPR	1.91 ± 0.45
TRAcP	319.57 ± 57.55
Cathepsin K	135.30 ± 36.25
Cathepsin D	−1.31 ± 0.30
Legumain	−1.84 ± 0.49
β-Glucuronidase	1.60 ± 0.31

[a] Average -fold change ratio in mRNA expression in Raw 264.7 cells *vs.* osteoclasts ($p < 0.05$).

metabolism. This demonstrates the complexity of the pool of Man-6-P glycoproteins secreted by osteoclasts, which is much higher than for other cell types such as monocytic or breast cancer cells where only ≈20 secreted proteins have been identified (19). So far, only the brain Man-6-P glycoproteome has been shown to consist of a comparable number of proteins (18).

Most of the proteins found in our analysis are known as typical lysosomal acid hydrolases targeted to lysosomes by a Man-6-P-dependent pathway in many other cell types (see Table I) (18, 20–24). Among these proteins, we detected the osteoclast marker cathepsin K thus proving the validity of our approach. In contrast, in a previous proteomic analysis of proteins secreted by osteoclasts that identified only a dozen proteins, this cathepsin was not found (25). In addition to well characterized Man-6-P-modified proteins we identified several lysosomal acid hydrolases, such as dipeptidyl-peptidase II, cathepsin Z, di-*N*-acetylchitobiase, and others, that are targeted to lysosomes by a yet unknown mechanism. Because the same enzymes isolated from brain tissue have also been found to interact *in vitro* with immobilized MPRs it is very likely that they contain the Man-6-P recognition marker (18). In contrast, β-glucosidase and lipoprotein lipase have been classified as enzymes following a Man-6-P-independent targeting pathway because they are reported as enzymes not being Man-6-P-modified (26, 27). Their detection among the Man-6-P-containing proteins in our screen could be explained in a way that a minor fraction of these enzymes might interact with other Man-6-P-containing ligands. This is underlined by the low abundance of these enzymes in our samples as indicated by the low number of detected peptides (see Table I). Finally we identified some proteins, namely sphingomyelinase-like phosphodiesterase 3a, interleukin-4-induced protein 1, and dentin matrix protein 4, that have not been found before to bind to immobilized MPRs. Secretion of these enzymes by osteoclasts might reflect their potential role in bone degradation.

A set of different acid hydrolases is required for the degradation of the organic bone matrix, mostly consisting of collagens, sulfated proteoglycans, and heavily sialylated glycoproteins such as osteocalcin or osteopontin. The substrate specificities of the acid hydrolases identified here would allow the digestion of these different components. Support of the notion comes from phenotypes observed in several naturally occurring human lysosomal storage disorders or in knock-out mice characterized by the monogenic defect of given acid hydrolases (see Table I). Accordingly several human lysosomal storage disorders are characterized by abnormalities of the skeleton (28). For example, mucopolysaccharidoses I, IIIA, B, D, IVA, and VI due to a deficiency in α-iduronidase, *N*-sulfoglucosamine sulfohydrolase, α-*N*-acetylglucosaminidase, *N*-acetylglucosamine-6-sulfatase, *N*-acetylgalactosamine-6-sulfatase, and arylsulfatase B, respectively, are all characterized by abnormal development of many bones including the spine and skeletal deformations such as thickened skulls or oval vertebrae (29). Similarly the Goldberg syndrome due to a lack of cathepsin A results in dwarfism (30). Sialidosis due to a lack of sialidase 1 is characterized in part by osteopenia (31). Some other enzyme deficiencies, not reported in humans, have been produced in animal models. For example, cathep-

sin K-deficient mice display an osteopetrotic phenotype, and cathepsin K-deficient osteoclasts exhibit a lower activity in bone degradation (32). Similarly cathepsin L-deficient mice have a lower trabecular, but not cortical, bone volume suggesting a role of this peptidase in bone development and turnover (33). In total, phenotypes of monogenetic defects concerning 33 of more than 50 acid hydrolases identified here to be secreted by osteoclasts are known. It is remarkable to note that 16 of them exhibit, as part of the phenotype, an etiology related to bone development and/or turnover. Some monogenic defects as seen for example in Niemann-Pick A, B, and C and infantile neuronal ceroid lipofuscinosis due to deficiencies in sphingomyelin phosphodiesterase, epididymal secretory protein E1, and palmitoyl-protein thioesterases 1 and 2, respectively, do not result in bone abnormalities. A simple explanation is that these enzymes involved in lipid metabolism might be less critical for bone metabolism than for other tissues such as brain. Moreover our analysis of acid hydrolases secreted by osteoclasts provides an exhaustive list of genes for which no natural occurring defect has been reported in humans or animals. Mouse genetics could be used to evaluate their functional importance in bone metabolism.

How acid hydrolases are secreted into the osteoclast resorption lacuna is largely unknown. From morphological studies examining the distribution of MPRs and acid hydrolases in osteoclasts, a constitutive pathway for enzyme transport toward the resorption lacuna has been proposed (7). However, the presence of late endosomal markers on the ruffled border membrane facing the resorption lacuna led to the proposal that late endocytic compartments could fuse with this membrane, resulting in the release of mature, fully active acid hydrolases (9, 11). Here we provide for the first time a biochemical study to address this question. Our data show that most of cathepsin K and about 50% of other acid hydrolases are secreted as Man-6-P-containing precursor forms. Moreover our immunoprecipitation experiments of cathepsin D demonstrate that this protease is exclusively secreted as proprotein. Therefore, our findings indicate that these enzymes have not encountered the acidic environment of late endocytic compartments where they would lose their Man-6-P markers and their prosequences. It is still unclear why a significant portion of the secreted acid hydrolases loses the Man-6-P modification resulting in the observed binding efficiency of about 50% to immobilized MPRs. This could simply reflect our incapability of efficiently blocking phosphatase activities and in particular TRAcP activity, which is also secreted in large amounts by osteoclasts and has been proposed to be involved in the dephosphorylation of Man-6-P recognition markers (34). Enhanced synthesis of MPRs as suggested by Baron *et al.* (7) does not seem to be the reason for increased routing of Man-6-P-containing acid hydrolases to the cell surface because we could not detect a drastic change in MPR expression. Moreover our findings also exclude a down-regulation of MPRs as explanation for the increased acid hydrolase secretion as has been described for cells lacking one of the two MPRs (35). It is also unlikely that an overload of the sorting capacity of the MPRs as observed in several cancer cells such as MCF-7 and CaCo-2 (36) causes the increased secretion of acid hydrolases by osteoclasts because none of the major secreted proteins are expressed at higher levels during osteoclastogenesis (see Fig. 3). In fact, only for the known osteoclast markers TRAcP and cathepsin K did we observe a highly increased expression in osteoclasts. Taken together, our data suggest that the secretion of acid hydrolases into the osteoclast resorption lacuna is caused by a modification of MPR trafficking pathways during osteoclastogenesis rather than by a fusion of acidic endocytic compartments containing fully processed enzymes with the ruffled border membrane. This is in accordance with previous studies showing changes in the steady state distribution of MPRs during the different phases of bone resorption (7, 9).[2] Further support for this notion comes from our studies of the intracellular localization of cathepsin D that led to the proposal of two different pools of this enzyme and possibly other acid hydrolases of which only the Man-6-P-containing pool is directly transported to the ruffled border. This is also consistent with our DNA microarray analysis of mRNA expression revealing that several effectors of GTPases of the ADP-ribosylation factor and Rab subfamilies functioning along the MPR and lysosomal membrane-associated glycoproteins transport routes are differentially regulated during osteoclastogenesis.[3] Further studies will address their implication in the polarized secretion of acid hydrolases by osteoclasts.

Acknowledgments—We thank Pierre Jurdic for reagents and advice concerning Raw 264.7 cell differentiation and Hella Hartmann for help with confocal microscopy.

* This work was supported in part by the Technical University of Dresden (Grant HWP-1207) and the Ministry of Research of Saxony (Grant SMWK-EFRE-1203). The costs of publication of this article were defrayed in part by the payment of page charges. This article must therefore be hereby marked "*advertisement*" in accordance with 18 U.S.C. Section 1734 solely to indicate this fact.

¶ To whom correspondence should be addressed: Technical University of Dresden-Bioinnovation Centre, Tatzberg 47-51, 01307 Dresden, Germany. Tel.: 49-351-463-40235; Fax: 49-351-463-40244; E-mail: bernard.hoflack@biotec.tu-dresden.de.

REFERENCES

1. Boyle, W. J., Simonet, W. S., and Lacey, D. L. (2003) Osteoclast differentiation and activation. *Nature* **423,** 337–342
2. Lacey, D. L., Timms, E., Tan, H. L., Kelley, M. J., Dunstan, C. R., Burgess, T., Elliott, R., Colombero, A., Elliott, G., Scully, S., Hsu, H., Sullivan, J., Hawkins, N., Davy, E., Capparelli, C., Eli, A., Qian, Y. X., Kaufman, S., Sarosi, I., Shalhoub, V., Senaldi, G., Guo, J., Delaney, J., and Boyle, W. J. (1998) Osteoprotegerin ligand is a cytokine that regulates osteoclast differentiation and activation. *Cell* **93,** 165–176
3. Väänänen, H. K., Zhao, H., Mulari, M., and Halleen, J. M. (2000) The cell

[2] C. Apfeldorfer and B. Hoflack, unpublished observations.
[3] H. Mansukoski and B. Hoflack, unpublished observations.

biology of osteoclast function. *J. Cell Sci.* **113,** 377–381
4. Blair, H. C., Teitelbaum, S. L., Ghiselli, R., and Gluck, S. (1989) Osteoclastic bone resorption by a polarized vacuolar proton pump. *Science* **245,** 855–857
5. Väänanen, H. K., Karhukorpi, E. K., Sundquist, K., Wallmark, B., Roininen, I., Hentunen, T., Tuukkanen, J., and Lakkakorpi, P. (1990) Evidence for the presence of a proton pump of the vacuolar H^+-ATPase type in the ruffled borders of osteoclasts. *J. Cell Biol.* **111,** 1305–1311
6. Ludwig, T., Le Borgne, R., and Hoflack, B. (1995) Roles for mannose-6-phosphate receptors in lysosomal enzyme sorting, IGF-II binding and clathrin-coat assembly. *Trends Cell Biol.* **5,** 202–206
7. Baron, R., Neff, L., Brown, W., Courtoy, P. J., Louvard, D., and Farquhar, M. G. (1988) Polarized secretion of lysosomal enzymes: co-distribution of cation-independent mannose-6-phosphate receptors and lysosomal enzymes along the osteoclast exocytic pathway. *J. Cell Biol.* **106,** 1863–1872
8. Baron, R., Neff, L., Louvard, D., and Courtoy, P. J. (1985) Cell-mediated extracellular acidification and bone resorption: evidence for a low pH in resorbing lacunae and localization of a 100-kD lysosomal membrane protein at the osteoclast ruffled border. *J. Cell Biol.* **101,** 2210–2222
9. Palokangas, H., Mulari, M., and Väänänen, H. K. (1997) Endocytic pathway from the basal plasma membrane to the ruffled border membrane in bone-resorbing osteoclasts. *J. Cell Sci.* **110,** 1767–1780
10. Toyomura, T., Murata, Y., Yamamoto, A., Oka, T., Sun-Wada, G. H., Wada, Y., and Futai, M. (2003) From lysosomes to the plasma membrane: localization of vacuolar-type H^+-ATPase with the a3 isoform during osteoclast differentiation. *J. Biol. Chem.* **278,** 22023–22030
11. Mulari, M. T. K., Zhao, H., Lakkakorpi, P. T., and Väänänen, H. K. (2003) Osteoclast ruffled border has distinct subdomains for secretion and degraded matrix uptake. *Traffic* **4,** 113–125
12. Czupalla, C., Mansukoski, H., Pursche, T., Krause, E., and Hoflack, B. (2005) Comparative study of protein and mRNA expression during osteoclastogenesis. *Proteomics* **5,** 3868–3875
13. Ludwig, T., Griffiths, G., and Hoflack B. (1991) Distribution of newly synthesized lysosomal enzymes in the endocytic pathway of normal rat kidney cells. *J. Cell Biol.* **115,** 1561–1572
14. Hoflack, B., and Kornfeld, S. (1985) Purification and characterization of a cation-dependent mannose 6-phosphate receptor from murine P388D1 macrophages and bovine liver. *J. Biol. Chem.* **260,** 12008–12014
15. Czupalla, C., Nürnberg, B., and Krause, E. (2003) Analysis of class I phosphoinositide 3-kinase autophosphorylation sites by mass spectrometry. *Rapid Commun. Mass Spectrom.* **17,** 690–696
16. Matsumoto, M., Sudo, T., Saito, T., Osada, H., and Tsujimoto, M. (2000) Involvement of p38 mitogen-activated protein kinase signaling pathway in osteoclastogenesis mediated by receptor activator of NF-κB ligand (RANKL). *J. Biol. Chem.* **275,** 31155–31161
17. Neufeld, E. F. (1991) Lysosomal storage diseases. *Annu. Rev. Biochem.* **60,** 257–280
18. Sleat, D. E., Lackland, H., Wang, Y., Sohar, I., Xiao, G., Li, H., and Lobel, P. (2005) The human brain mannose 6-phosphate glycoproteome: a complex mixture composed of multiple isoforms of many soluble lysosomal proteins. *Proteomics* **5,** 1520–1532
19. Journet, A., Chapel, A., Kieffer, S., Roux, F., and Garin, J. (2002) Proteomic analysis of human lysosomes: application to monocytic and breast cancer cells. *Proteomics* **2,** 1026–1040
20. Sleat, D. E., Donnelly, R. J., Lackland, H., Liu, C. G., Sohar, I., Pullarkat, R. K., and Lobel, P. (1997) Association of mutations in a lysosomal protein with classical late-infantile neuronal ceroid lipofuscinosis. *Science* **277,** 1802–1805
21. Sleat, D. E., Sohar, I., Lackland, H., Majercak, J., and Lobel, P. (1996) Rat brain contains high levels of mannose-6-phosphorylated glycoproteins including lysosomal enzymes and palmitoyl-protein thioesterase, an enzyme implicated in infantile neuronal lipofuscinosis. *J. Biol. Chem.* **271,** 19191–19198
22. Wiederanders, B., Bromme, D., Kirschke, H., von Figura, K., Schmidt, B., and Peters, C. (1992) Phylogenetic conservation of cysteine proteinases. Cloning and expression of a cDNA coding for human cathepsin S. *J. Biol. Chem.* **267,** 13708–13713
23. Ullrich, K., Basner, R., Gieselmann, V., and von Figura, K. (1979) Recognition of human urine α-N-acetylglucosaminidase by rat hepatocytes. Involvement of receptors specific for galactose, mannose 6-phosphate and mannose. *Biochem. J.* **180,** 413–419
24. Bielicki, J., Hopwood, J. J., Melville, E. L., and Anson, D. S. (1998) Recombinant human sulphamidase: expression, amplification, purification and characterization. *Biochem. J.* **329,** 145–150
25. Kubota, K., Wakabayashi, K., and Matsuoka, T. (2003) Proteome analysis of secreted proteins during osteoclast differentiation using two different methods: two-dimensional electrophoresis and isotope-coded affinity tags analysis with two-dimensional chromatography. *Proteomics* **3,** 616–626
26. Owada, M., and Neufeld, E. F. (1982) Is there a mechanism for introducing acid hydrolases into liver lysosomes that is independent of mannose 6-phosphate recognition? Evidence from I-cell disease. *Biochem. Biophys. Res. Commun.* **105,** 814–820
27. Friedman, G., Chajek-Shaul, T., Olivecrona, T., Stein, O., and Stein, Y. (1982) Fate of milk ^{125}I-labelled lipoprotein lipase in cells in culture. Comparison of lipoprotein lipase- and non-lipoprotein lipase-synthesizing cells. *Biochim. Biophys. Acta* **711,** 114–122
28. Vellodi, A. (2004) Lysosomal storage disorders. *Br. J. Haematol.* **128,** 413–431
29. Spranger, J. W. (1977) Catabolic disorders of complex carbohydrates. *Postgrad. Med. J.* **53,** 441–449
30. Goldberg, M. F., Cotlier, E., Fichenscher, L. G., Kenyon, K., Enat, R., and Borowsky, S. A. (1971) Macular cherry-red spot, corneal clouding, and β-galactosidase deficiency. Clinical, biochemical, and electron microscopic study of a new autosomal recessive storage disease. *Arch. Intern. Med.* **128,** 387–398
31. Spranger, J. W., Gehler, J., and Cantz, M. (1977) Mucolipidosis I—a sialidosis. *Am. J. Med. Genet.* **1,** 21–29
32. Saftig, P., Hunziker, E., Wehmeyer, O., Jones, S., Boyde, A., Rommerskirch, W., Moritz, J. D., Schu, P., and von Figura, K. (1998) Impaired osteoclastic bone resorption leads to osteopetrosis in cathepsin-K-deficient mice. *Proc. Natl. Acad. Sci. U. S. A.* **95,** 13453–13458
33. Potts, W., Bowyer, J., Jones, H., Tucker, D., Freemont, A. J., Millest, A., Martin, C., Vernon, W., Neerunjun, D., Slynn, G., Harper, F., and Maciewicz, R. (2004) Cathepsin L-deficient mice exhibit abnormal skin and bone development and show increased resistance to osteoporosis following ovariectomy. *Int. J. Exp. Pathol.* **85,** 85–96
34. Bresciani, R., and von Figura, K. (1996) Dephosphorylation of the mannose-6-phosphate recognition marker is localized in later compartments of the endocytic route. Identification of purple acid phosphatase (uteroferrin) as the candidate phosphatase. *Eur. J. Biochem.* **238,** 669–674
35. Ludwig, T., Munier-Lehmann, H., Bauer, U., Hollinshead, M., Ovitt, C., Lobel, P., and Hoflack, B. (1994) Differential sorting of lysosomal enzymes in mannose 6-phosphate receptor-deficient fibroblasts. *EMBO J.* **13,** 3430–3437
36. Kokkonen, N., Rivinoja, A., Kauppila, A., Suokas, M., Kellokumpu, I., and Kellokumpu, S. (2004) Defective acidification of intracellular organelles results in aberrant secretion of cathepsin D in cancer cells. *J. Biol. Chem.* **279,** 39982–39988